

Decomposition of solid explosives by laser irradiation: a mass spectrometric study

TONG B. TANG*, M. M. CHAUDHRI, CAROLINE S. REES
Cavendish Laboratory, Madingley Road, Cambridge CB3 0HE, UK

S. J. MULLOCK†
Department of Metallurgy and Materials Science, University of Cambridge, Pembroke Street, Cambridge CB2 3QZ, UK

Experimental investigations have been made in which single crystals of solid explosives such as cyclotrimethylene trinitramine, RDX, pentaerythritol tetranitrate, PETN, AgN_3 and $\text{Pb}(\text{N}_3)_2$, were irradiated with a focused laser beam of wavelength 266 nm and duration ~ 5 nsec in an ultra high vacuum system housing a fast and sensitive time-of-flight mass spectrometer. From the mass spectra (both +ve and -ve ions) of the chemical species obtained, possible decomposition schemes of RDX and PETN have been proposed. For silver and lead azides, the laser irradiation did not cause explosions if the power density was sufficiently low, but micrometre size craters were formed. In the mass spectra of AgN_3 products N_3^- and silver cluster ions, Ag_n^+ , have been found for the first time. It has been suggested that such investigations may possibly throw some light on our understanding of the reactions taking place in a deflagration/detonation wave.

1. Introduction

The use of focused laser beams in conjunction with mass spectrometry has proven valuable in the micro-analysis of materials and the study of decomposition of solids over the past two decades [1]. Nearly ten years ago, a commercial instrument became available which combined a laser induced ionization source with a time-of-flight spectrometer under the generic name LAMMA, standing for laser microprobe mass analyser. These early machines all worked in the transmission or grazing incidence modes with the laser and mass spectrometer on opposite sides of the sample. More recently, a new commercial system has been developed which is capable of analysis in the reflection mode and therefore suitable for the analysis of bulk samples [2]. The system is called LIMA, an acronym for "laser ionization mass analyser". An important feature of this system is that ionized species are formed by the laser pulse alone.

The use of a Q-switched laser beam of the LIMA allows us to produce very localized heating in a region of diameter 1 to 3 μm to very high temperatures in a short time of ~ 5 nsec. Such high temperature conditions prevail in a detonation wave in which pressures of up to several hundred kbar may exist. The incident laser beam can also cause localized high pressures of magnitude of tens of kbar [3], and therefore the LIMA technique is especially attractive in possibly providing a simple laboratory method for studying the decomposition of reactive materials under conditions of transient high temperatures and pressures.

Our investigations have shown that the LIMA can be successfully employed for studying reactive materials and the findings from experiments on explosives such as RDX, PETN, AgN_3 and $\text{Pb}(\text{N}_3)_2$ are reported below.

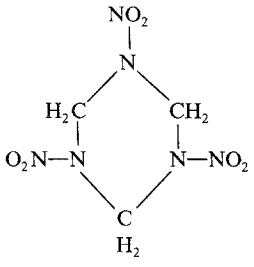
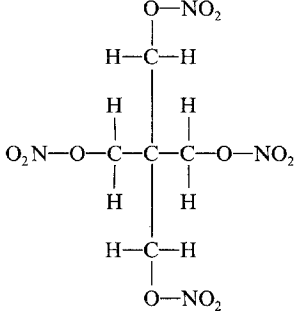
2. Experimental procedures

The experiments were carried out under ultra high vacuum conditions in a LIMA model 2A (Cambridge Mass Spectrometry Ltd) of the Department of Metallurgy and Materials Science of this university. The instrument incorporates a Q-switched Nd: YAG laser; its beam is frequency quadrupled to give a pulse of ~ 5 nsec in duration at a wavelength of 266 nm. The maximum output energy of the laser at this wavelength is up to 20 mJ but that reaching the target is only up to $\sim 500 \mu\text{J}$. The power density at the target can be varied in the range 10^9 to $10^{11} \text{ W mm}^{-2}$ by defocusing the laser spot. The ions produced from the irradiated spot (diffraction limited diameter: 1 μm) on the target surface are immediately accelerated by a potential fall of +3 kV or -3 kV over a distance of 14 mm, before going into the field-free drift tube, 2 m in length. This means that the time required to extract an ion of 1 atomic mass unit (a.m.u.) from the field region is ~ 40 nsec, whereas it is ~ 400 nsec for an ion of 100 a.m.u. Therefore, if there is no fragmentation of the ions during their passage through the field-free drift tube, the recorded mass spectra will represent the products which existed within a microsecond of their formation at the sample surface.

*Permanent address: Department of Physics, Hong Kong Baptist College, 224 Waterloo Road, Kowloon, Hong Kong.

†Present address: Cambridge Mass Spectrometry Ltd, Cambridge Science Park, Milton Road, Cambridge CB4 4FX, UK.

TABLE I Chemical formulae of the various explosives

Explosive	Chemical formula
Cyclotrimethylene trinitramine (RDX)	
Pentaerythritol tetranitrate (PETN)	
Lead azide	$(\text{N}=\text{N}=\text{N})^- \text{Pb}^{++} (\text{N}=\text{N}=\text{N})^-$
Silver azide	$\text{Ag}^+ (\text{N}=\text{N}=\text{N})^-$

There is an electrostatic reflecting element at the end of the drift tube, which provides a correction for the spread in the initial energy of the ions. The mass resolving power of the instrument is better than 500 FWHM (full width half maximum) and the time spectrum of the ionic current, obtained over a period of up to 100 μsec , is digitized and stored on a computer. A detailed description of the instrument may be found elsewhere [2].

The materials investigated were: (1) cyclotrimethylene trinitramine, RDX, (2) pentaerythritol tetranitrate, PETN, (3) silver azide, and (4) α - and β -lead azides. The chemical formulae of the materials are given in Table I. RDX and PETN are commonly-used secondary explosives, while the other two are primaries and are extensively used in the initiator devices as detonants. Single crystals of RDX, 3 to 4 mm across, were obtained by slow cooling of its solution in analar acetone at 70°C to room temperature, whereas single crystals of PETN of a similar size were prepared by slow evaporation of its saturated solution in analar acetone at room temperature. Single crystals of silver azide of size 100 μm \times 100 μm \times 10 mm were recrystallized from its solution in ammonia, whereas lead azide crystals of similar dimensions were grown by a diffusion method.

For analysis in the LIMA, the crystal under study was mounted on a metallic stud with a piece of double-sided adhesive tape. A fine wire stainless steel mesh, in electrical contact with the stud, lightly pressed on to the crystal, covering it completely. This mesh was necessary in order to avoid distorting the ion optics in the extraction region due to the electrical charging of the crystal surface during the laser irradiation.

The impact of the focused Q-switched laser beam caused craters in all specimens. Moreover, RDX and PETN showed some cracking around the craters. The damage was first photographed under an optical

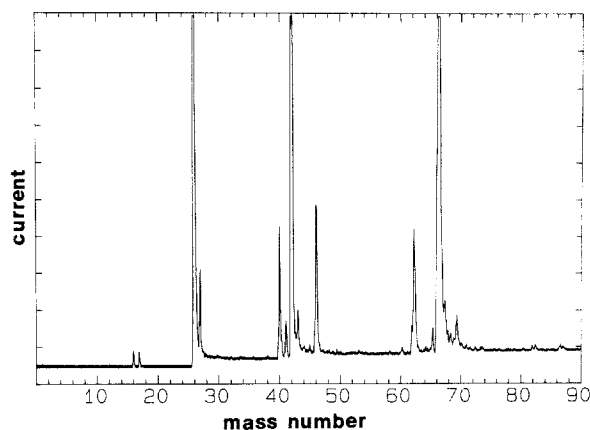


Figure 1 Negative ion mass spectrum of RDX. Small peaks exist for $m = 125$ and 134 , but have not been shown.

microscope within 2 h of the irradiation. The specimens were then coated with a thin film of silver or gold and examined in a scanning electron microscope (Cambridge Stereoscan 250 mk 2).

3. Results

Representative results from the LIMA experiments are presented in Figs 1 to 6, which plot ionic current (either negative or positive) against mass number (all ions have been assumed to be singly charged and the identification of the peaks has been done according to the corresponding mass and the structure of the parent molecule). For this very short time in which the mass spectra are taken, it is not possible to give a thermodynamically stable charge distribution on the products. We first consider RDX (Fig. 1). The detected species can be identified as the negative ions of O, OH, CN, HCN, NCN, N(HC)N, N(H₂C)N and NO₂ for mass numbers 16, 17, 26, 27, 40, 41, 42 and 46, respectively.

For peaks at higher mass numbers, the assignment becomes ambiguous and uncertain. The one at $m = 62$ could be due to NO₃; that at 65 can possibly be due to CN(HC)NC; and that at 66 may be CN(H₂C)NC and/or C₂N₃. At still higher mass numbers peaks occur for $m = 86, 90, 93$ and $98, 134$ and 176 , which, excepting $m = 90$, may be due to the ions (CH₂)₂N-NO₂, (CH)(NCNC)(NN), (CH₂)₃N₂(NN), H₂C(N-NO₂)₂ and (CH₂)₃(N-NO₂)₂N, respectively.

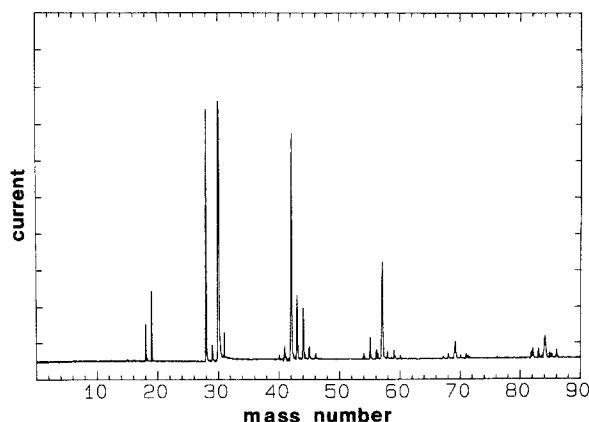


Figure 2 Positive ion mass spectrum of RDX. Small peaks at 125 and 130 have not been shown.

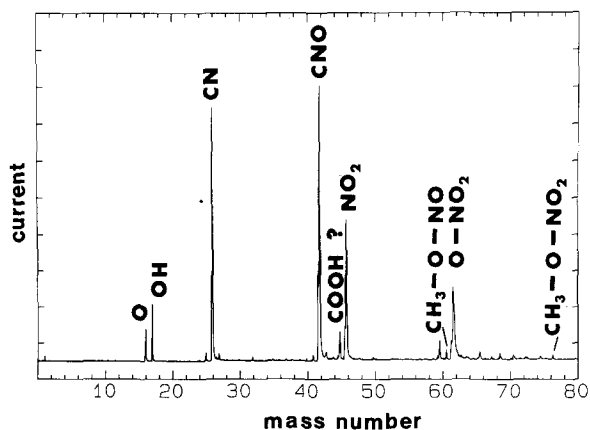


Figure 3 Negative ion mass spectrum of PETN.

In the positive ion spectrum of RDX (Fig. 2), the peaks for $m = 18, 19, 28, 30$ and 42 can be attributed to H_2O , H_3O^+ , CO^+ and/or N_2^+ , NO^+ , and $(\text{H}_2\text{C})_2\text{N}^+$, respectively. The peaks at $57, 69$ and 84 may plausibly be assigned to HCNNO^+ , $(\text{H}_2\text{C})\text{N}(\text{CH}_2)\text{N}(\text{CH})^+$ and $(\text{H}_2\text{CN})_3^+$, respectively.

Small peaks at $82, 83, 85$ and 86 may be due to $(\text{HC})\text{N}(\text{CH})\text{N}(\text{CH}_2)\text{N}^+$, $(\text{HC})\text{N}(\text{H}_2\text{C})\text{N}(\text{H}_2\text{C})\text{N}^+$, $\text{C}(\text{CH})\text{N}-\text{NO}_2^+$ and $(\text{CH})_2\text{N}-\text{NO}_2^+$. At still higher mass numbers peaks exist at $m = 98, 125$ and 130 . The one at 130 is likely to be $(\text{H}_2\text{C})\text{N}(\text{CH}_2)\text{N}(\text{CH}_2)(\text{N}-\text{NO}_2)^+$, which loses two oxygens to give $m = 98$. The peak at $m = 125$ may be due to $(\text{HC})(\text{NCNC})(\text{N}-\text{NO}_2)^+$.

The results from PETN experiments for $-ve$ and $+ve$ ions are shown in Figs 3 and 4, respectively. For the $-ve$ ions, the peaks occur at $m = 16, 17, 25, 26, 27, 32, 41, 42, 43, 44, 60, 61, 65, 68, 69, 71, 75$ and 77 ; for the $+ve$ ions, the peaks are at $m = 12, 13, 14, 15, 16, 17, 18, 19, 24, 26, 27, 28, 29, 30, 32, 44$ and 45 . Some of the peaks have been identified in the figures and others in Table II.

In the case of silver azide crystals it was found that relatively moderate power densities caused explosions. However, for lower power densities there were no explosions, though decomposition products were formed. A negative ion mass spectrum obtained when a crystal was irradiated for the fifth time at one site on the crystal surface is shown in Fig. 5. Major peaks occur at $m = 42, 107, 109$ corresponding to N_3^- , ^{107}Ag and ^{109}Ag , respectively. For higher power densities, N_2^- is also observed (not shown here). The positive ion

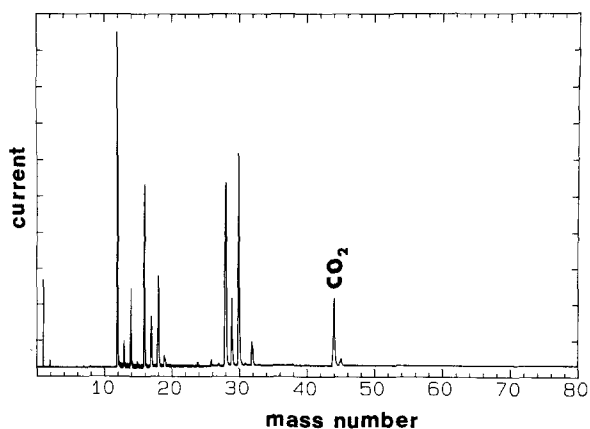


Figure 4 Positive ion mass spectrum of PETN.

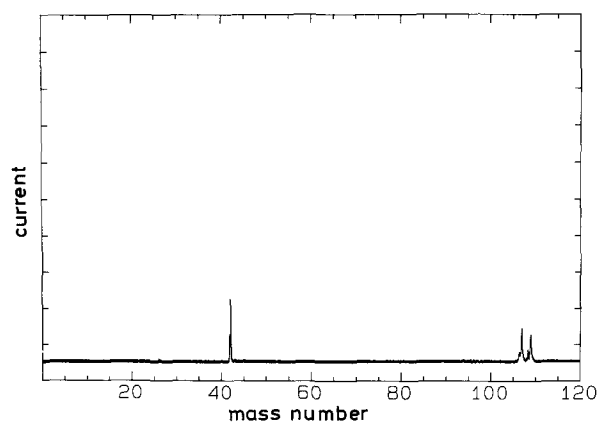


Figure 5 Negative ion mass spectrum of AgN_3 .

spectra showed some very interesting features: silver cluster ions, Ag_n^+ , were formed with a n value of up to 7, and the signal height for an even value of n was considerably smaller than that for an odd value. A typical spectrum is shown in Fig. 6. Such clusters were not observed when a piece of pure silver metal was irradiated with the laser beam, other conditions being similar. However, Katakuse *et al.* [4] have reported that when metallic silver is bombarded with 10 keV Xe^+ ions, clusters, Ag_n^+ , of silver are formed. They also found that the intensity of odd n clusters was greater than that for even.

In our previous studies [5] on β -lead azide single crystals we found that for a Q-switched unfocused ruby laser beam ($\lambda = 694.3 \text{ nm}$) of duration 80 nsec , energy 0.5 mJ , and a power density of $1.9 \times 10^2 \text{ W mm}^{-2}$ initiation of an explosion occurred with a probability of 50%. Therefore, for this work we used as low a power density as was conveniently possible with the LIMA instrument. The magnitude of this power density was, however, not measured. Furthermore, to safeguard the sensitive instrumentation, the mass spectrometer was not operated lest an unwanted explosion occurred. It was generally observed that on the first irradiation of an α - or β -lead azide crystal an explosion did not occur, but some cratering of the surface did occur. However, when the irradiation was allowed to take place a second time on a site which had been irradiated once before, the probability of the initiation of an explosion was much higher.

The microscopical examination of the samples

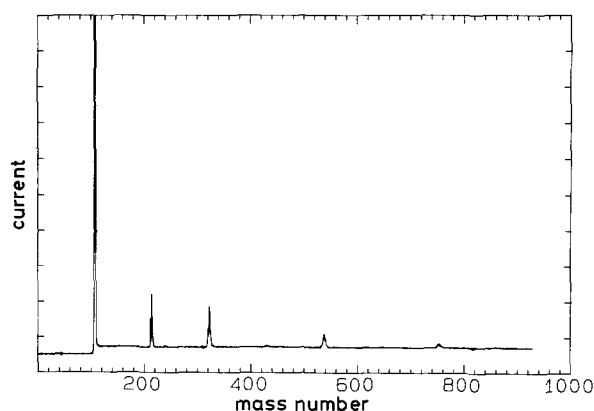


Figure 6 Positive ion mass spectrum of AgN_3 .

TABLE II Comparison of PETN detonation products with those formed in LIMA

Atomic mass unit of species	Chemical formula	Relative intensities of the products with that of CO ₂ as unity		
		Höh and Aulinger [17]	Blais and Valentini [18]	LIMA (This work)
1	H	0.3	0.6	1.2
2	H ₂	0.6	0	0.1
12	C	0.3	0.3	4.5
13	CH	0	0	0.3
14	N	0.2	0.2	1
15	CH ₃	0	0.3	0.05
16	O	0.4	0.8	2.5
17	OH	0.6	1	0.7
18	H ₂ O	2	≥ 6	1.3
19	H ₃ O	0	0	0.05
24	C ₂	0	0	0.05
26	C ₂ H ₄	0	0	0.1
27	HCN	0.2	0.1	0.05
28	CO/N ₂	8	1.2	2.6
29	HCO	0.6	0.2	1
30	NO/HCHO	1	0.5	3
32	O ₂	0.6	0	0.4
42	CNO	0.15	0	0
44	CO ₂	1	1	1
45	HN ₂ O(?)	0.05	0	0.1
46	NO ₂	0.05	0.6	0
> 46	—	0	0	0

revealed that at the irradiation site a central crater of diameter 3 to 5 μm formed within a larger but shallower crater of about 15 to 20 μm in diameter. Moreover, the central crater was 4 to 5 μm deep. It is interesting to note that the material within the craters did not appear to have melted. This is in contrast to the observations made by Southon *et al* [2] in which evidence for melting was quite clear for targets such as a stainless steel and a nickel-based superalloy. Electron micrographs of typical craters in PETN and RDX are shown in Figs 7a and b, respectively. It will also be seen that within the shallower craters in both these explosives the material has become of particulate nature. This could be due to very rapid vaporization and decomposition at the irradiated site.

The systems of cracks around the craters are reminiscent of those formed by localized loading as, for example, in the case of ionic crystals impacted by

microparticles [6]. In this work, the loading is probably due to the rapid ejection of the surface material. It may also be pointed out that no slip traces were observed around the craters; this contrasts with the observations made from static loading of crystals of these materials with a pointed diamond indenter [7]. A possible contributory factor for these differences may be the very high strain rates prevalent in the laser irradiation experiments.

For silver azide and lead azide crystals as well, cratering and cracking occurred; micrographs of the craters are shown in Figs 8a and b.

4. Discussion

The laser beam of the LIMA ($\lambda = 266 \text{ nm}$) is smaller than the absorption edge wavelength of all the explosives examined here [8]. Therefore the incident focused beam is likely to be absorbed completely in a layer

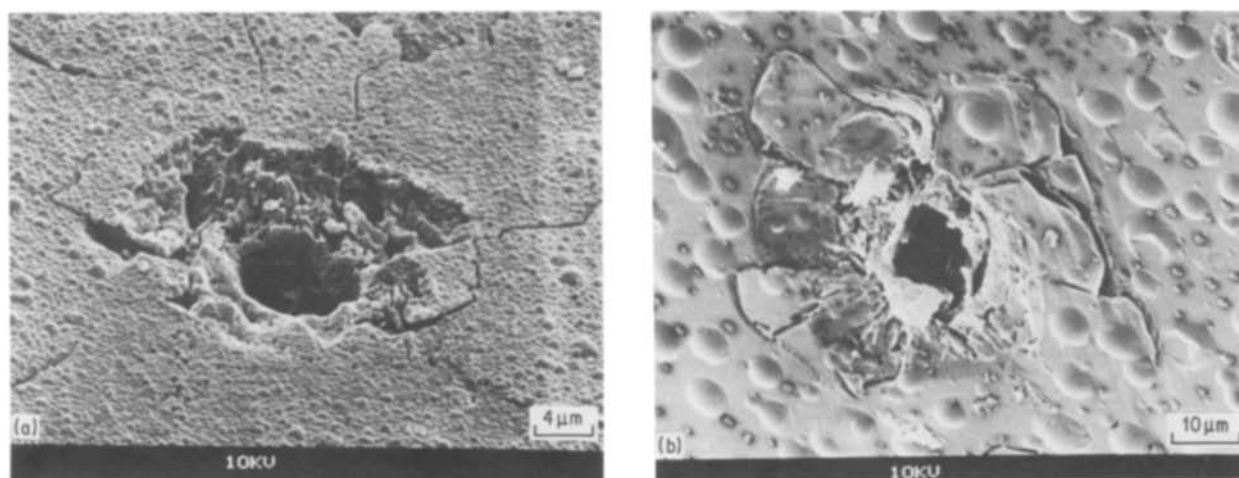


Figure 7 Scanning electron micrographs of the laser-generated craters in (a) RDX, and (b) PETN.

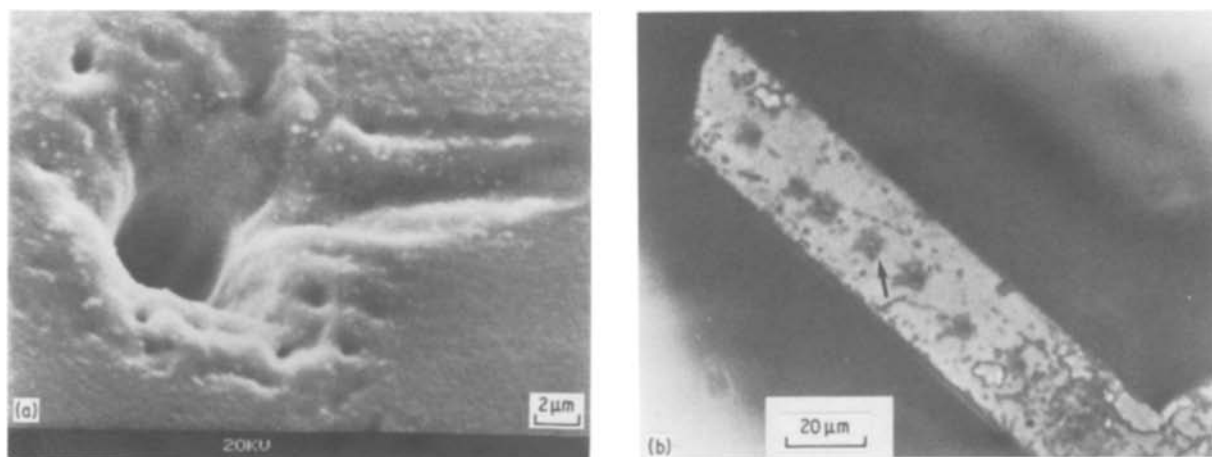


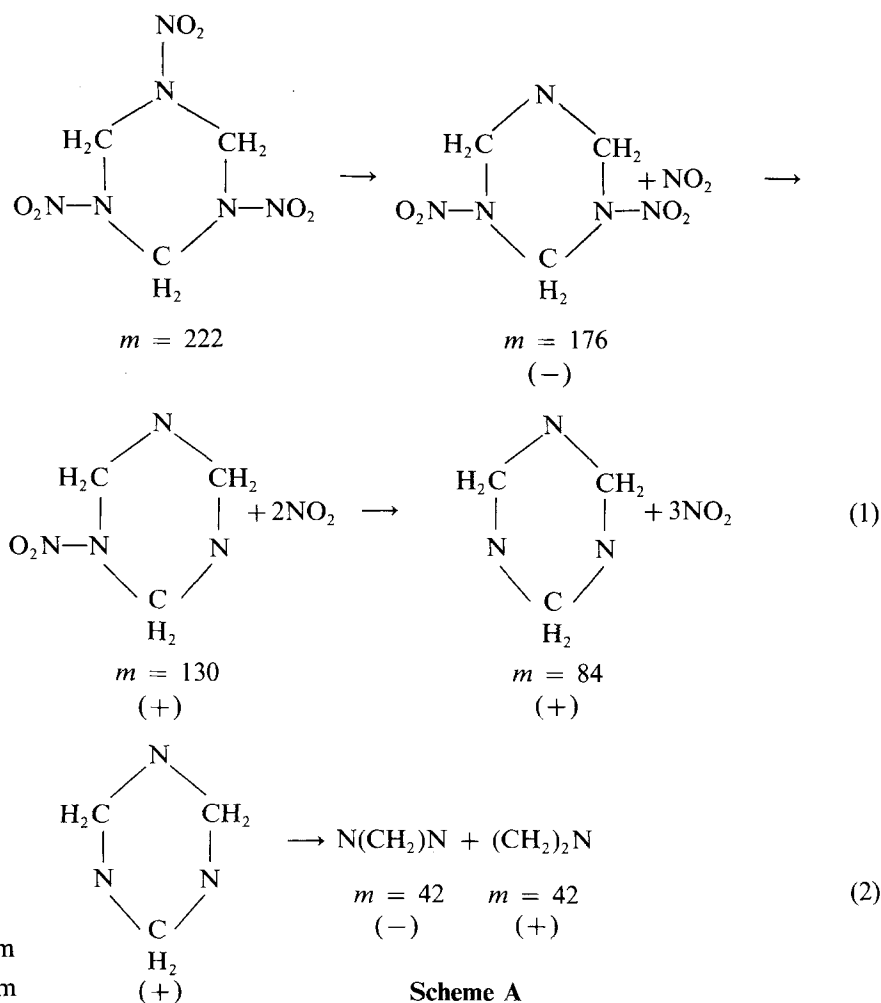
Figure 8 Laser-generated craters in (a) AgN_3 (scanning electron micrograph), and (b) $\alpha\text{-PbN}_6$ (optical micrograph, the arrow indicating a crater).

only a few micrometers thick. The melting points of RDX, PETN and AgN_3 are 205, 140 and 305°C respectively; lead azide does not melt [9]. Simple calculations show that all these materials (except lead azide) will have reached the melting points during the irradiation. It is probable that the temperatures at the irradiation sites are much higher, and rough estimates indicate that temperatures of the order of 10^5 K will have been reached. Under these conditions, the hot material (molten/vaporous) will be ejected from the surface at velocities of up to km sec^{-1} , causing impulsive localized loading and high transient pressures. It would appear, therefore, that the decomposition

occurring in LIMA possibly has some similarities of conditions to those in deflagration and detonation wavefronts. We shall discuss separately the results from the different materials.

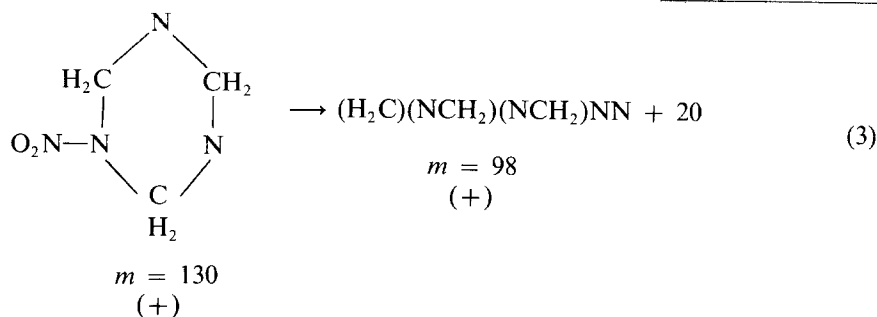
4.1. RDX

From the mass spectra presented in Section 3, along with the identification of the peaks, we believe there are at least three different possible schemes for the breakdown of the RDX molecule. In one, as initial steps, there is successive loss of the nitrogroups (scheme A).

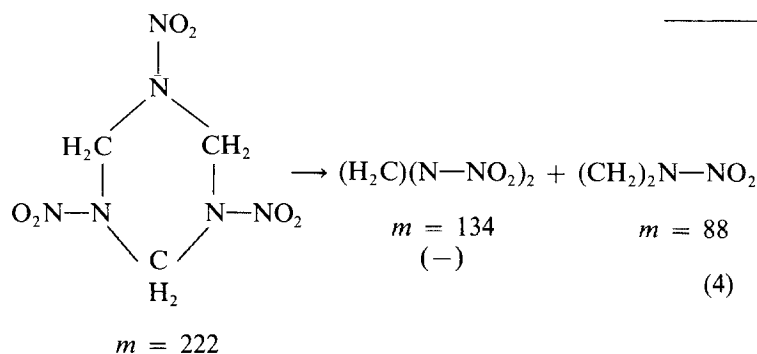


(-) detected in -ve ion spectrum
 (+) detected in +ve ion spectrum

The observed peaks at $m = 176$, 130 and 84 support this sequence of the breakdown. After the loss of the nitrogroups, two C–N bonds of the ring break to produce two products of equal mass 42 (step 2). These products then further degrade to give peaks at $m = 26$, 27 and 28. It also appears that after the loss of two nitrogroups by the RDX molecule the remainder nitrogroup on the ring loses its two oxygens to give $m = 98$ (scheme B).



Further loss of H will give rise to peaks between 92 and 97. However, only peaks at 93 and 96 have been observed. A third scheme of the breakdown also seems to occur (scheme C).



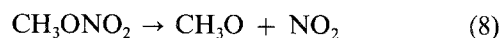
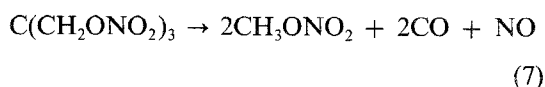
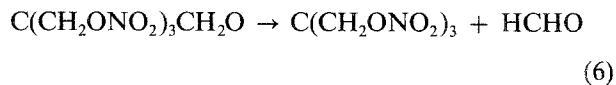
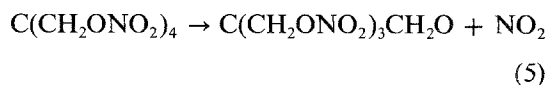
In this, two C–N bonds of the RDX molecule break up first to give two fragments $(\text{CH}_2)_2\text{N}-\text{NO}_2$ and $\text{N}-\text{NO}_2(\text{CH}_2)_2\text{N}-\text{NO}_2$ of mass numbers 88 and 134, respectively. The latter has been observed in this work; the heavier fragment then first loses a nitrogroup and then two hydrogens to give $\text{O}_2\text{N}-\text{N}-\text{C}-\text{N}$ of $m = 86$, which has also been observed. The lighter fragment breaks down by losing CH_2 groups to give $\text{N}-\text{NO}_2$ ($m = 60$); NO_2 may pick up an oxygen to give NO_3 . Both peaks at $m = 60$ and $m = 62$ have been observed.

It is interesting to note that several of the products monitored in this work were not reported in an earlier study [10], though in that, the products were examined by chemical gas analysis. Moreover, we did not observe any nitroso derivatives of RDX (i.e. loss of an oxygen from the nitrogroups) whose existence has been reported in the products of the thermal [11] and impact-initiated decompositions [12].

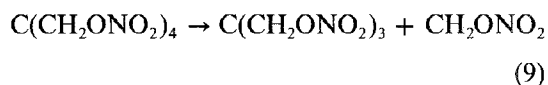
4.2. PETN

The products of slow thermal decomposition of this

material have been analysed by Fox and Soria-Ruiz [13] and by Ng *et al.* [14]. The latter group have put forward the early steps of the thermal degradation as:



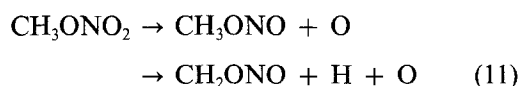
On the other hand, when the decomposition was caused by the propagation of a fast fracture in a single crystal of PETN the products were different and the proposed reaction scheme [15] is:



The $\text{C}(\text{CH}_2\text{ONO}_2)_3$ radical presumably disintegrates to give methyl nitrate ($m/e = 77$) and then CH_3O ($m/e = 31$), etc., as proposed before (steps 7 and 8). On decomposition by a ruby laser pulse of wavelength 694.3 nm, duration 20 nsec and power density 10^8 W mm^{-2} , the initial step has been proposed to be the cleavage of either the $\text{CH}_2\text{O}-\text{NO}_2$ bond or the CH_2-ONO_2 bond, both alternatives occurring in competition [16].

Our LIMA results shown in Figs 3 and 4 are consistent with the proposal in [15]. The species NO_2^- , HCHO^+ (possibly) along with ONO_2^- are present in our spectra. Concerning the step (8) however, in our

studies CH_3O has not been detected. On the other hand, as shown in Fig. 3, definite peaks exist at $m/e = 61$ and 60 . We therefore suggest that instead of following the proposed step (8), methyl nitrate ion decomposes thus:



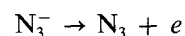
It is interesting to compare the products of decomposition formed in our LIMA studies with those formed by detonating PETN charges [17, 18]. This comparison is shown in Table II; here we have normalized the intensities by taking that of CO_2 as 1. It will be seen from the table that there are several near similarities in the products formed by the different techniques. For example, the number of species detected for $m < 47$ is 19 from the LIMA experiments and 13 and 16 from the other works. Moreover, the intensity of species (negative ions) for $m > 46$ is negligible for all three types of investigation. Also, the species identified in this work agree reasonably well with those in the other investigations. There are, however, some notable differences. For example, in the LIMA experiments C is the strongest peak, whereas Blais and Valentini [18] find H_2O as the strongest peak, and H6h and Aulinger [17] give CO_2/N_2 as the most abundant product. It is possible that these differences are not of fundamental type (i.e. the types of decomposition products formed by the two techniques), but appear on account of the detection sensitivity and time resolution of the instruments employed. Another contributory factor could be the fact that the other two research groups ionized the reaction products with an electron beam before mass analysis, whereas in the LIMA the ionization takes place due to the laser beam irradiation alone.

4.3. Silver azide

The formation of craters (Fig. 8) in a single crystal of silver azide due to the laser beam irradiation is a surprising observation, as it is generally thought that if conditions of self-heating take place in this material in a microscopic region, an explosion of the entire sample takes place. It may be argued that the size of the heated volume is below the required minimum value [8]. However, our earlier experiments [19, 20] have shown that this minimum size of the heated zone may be sub-micrometer. It is possible that since the laser pulse is ~ 5 nsec in duration, the hot material leaves the crystal surface before any significant exothermic reaction occurs.

The negative ion mass spectrum of silver azide (Fig. 5) shows peaks at mass numbers 42, 107 and 109. The latter two represent the two stable isotopes of silver and the one at 42 is identified as N_3^- ; the amount of N_3^- detected is about 1/10th of the total amount of the +ve and -ve ions of silver. This is the first time that N_3^- has been observed in the degradation of AgN_3 (or any other inorganic azide), though the formation of N_3 radical has been postulated as one of the intermediate steps leading to the final degradation by Bartlett *et al.* [21]. According to them, the primary

step during the thermal decomposition of silver azide is the excitation of an electron to the conduction band of the solid. That is, the electron is removed from the azide ion in the solid to form a neutral azide radical:



At present we do not know whether the observed N_3^- is formed after the formation of the N_3 neutral or whether it is a consequence of the breakage of the ionic bond between the silver and nitrogen in the solid state by the laser beam.

The formation of silver ion clusters is another interesting observation (Fig. 6). It supports the mechanism [22] for the development of metallic silver during the thermal decomposition of AgN_3 . According to this mechanism, metallic nuclei grow by the addition of individual interstitial silver ions to negatively charged metal specks. However, at present we do not know why Ag_n^+ clusters have relatively low intensity for an even value of n .

4.4. Lead azide

Lead azide is not known to melt before explosion [9]. Whether any melting occurs during the laser irradiation cannot be ascertained. However, the craters formed (Fig. 8b) do not suggest that any melting took place. It is again very surprising that though craters are formed in this sensitive material, initiation of fast reaction does not occur at relatively low power densities of the laser beam. Again a possible explanation is that proposed above for silver azide.

5. Conclusions

It has been shown that LIMA (i.e. laser ionization mass analysis) can be successfully employed in studying the rapid (but not self-sustained) decomposition of both secondary and primary explosives under conditions of high temperatures and high pressures (possibly tens of kbar). From the measured m/e of the decomposition products the reaction steps of the various explosive materials have been proposed. Moreover, it has been suggested that this technique of investigating the decomposition of energetic materials may possibly be suitable for studying the decomposition processes which occur in a deflagration/detonation wave. Another advantage of this technique is that since the laser-irradiated area is only of $10 \mu\text{m}$ or less in diameter, it is particularly suitable for micro-analysis of explosive materials of composite nature. The laser beam used in this work is in the ultraviolet region and, being below the absorption edge of these materials, is heavily absorbed in a thin surface layer. It would be interesting to use longer wave lengths for further work.

N_3^- ions have been shown to exist in the products of AgN_3 . It would also be interesting to see whether N_3 can be formed by the laser irradiation of other inorganic azides, such as KN_3 .

Acknowledgements

We should like to thank Drs A. D. Yoffe and O. Nehme of the Cavendish Laboratory for critical comments on the manuscript. The work was supported by

grants from the Ministry of Defence, UK (Procurement Executive) and the US Government through its European Office.

References

1. R. J. COMZEMIUS and J. M. CAPELLEN, *Int. J. Mass Spectrom. Ion Phys.* **54** (1980) 197.
2. M. J. SOUTHON, M. C. WITT, A. HARRIS, E. R. WALLACH and J. MYATT, *Vacuum* **34** (1984) 903.
3. C. H. SKEEN and C. M. YORK, *Appl. Phys. Lett.* **12** (1968) 369.
4. I. KATAKUSE, T. ICHIHARA, F. FUJITA, T. MATSUO, T. SAKURI and H. MATSUDA *Int. J. Mass Spectrom. and Ion Processes* **67** (1985) 229.
5. J. T. HAGAN and M. M. CHAUDHRI, *J. Mater. Sci.* **16** (1981) 2457.
6. M. M. CHAUDHRI, J. K. WELLS and A. STEPHENS, *Phil. Mag.* **A43** (1981) 643.
7. J. T. HAGAN and M. M. CHAUDHRI, *J. Mater. Sci.* **12** (1977) 1055.
8. F. P. BOWDEN and A. D. YOFFE, "Fast Reactions in Solids" (Butterworths, London, 1958)
9. M. M. CHAUDHRI and J. E. FIELD, *J. Solid State Chem.* **12** (1975) 72.
10. A. J. B. ROBERTSON and A. D. YOFFE, *Nature* **161** (1948) 806.
11. J. C. HOFFSOMMER and D. J. GLOVER, *Combustion & Flame* **59** (1985) 303.
12. J. SHARMA, J. C. HOFFSOMMER, D. J. GLOVER, C. S. COFFEY, J. W. FORBES, T. P. LIDDIARD, W. L. ELBAN and F. SANTIAGO, Preprint of the 8th Symposium (International) on Detonation, Albuquerque, New Mexico, USA, July 1985 (Lawrence Livermore, National Laboratory, USA, 1985) Vol. 3, p. 931.
13. P. G. FOX and J. SORIA-RUIZ, *Proc. R. Soc.* **A317** (1970) 79.
14. W. L. NG, J. E. FIELD and H. M. HAUSER, *J. C. S. Perkin Trans. II* 637 (1976).
15. H. M. HAUSER, J. E. FIELD and V. KRISHNA MOHAN, *Chem. Phys. Lett.* **99** (1983) 66.
16. W. L. NG, J. E. FIELD and H. M. HAUSER, submitted to *J. Appl. Phys.* **59** (1986) 3945.
17. A. HÖH and F. AULINGER, *Dyn. Mass Spectrom.* **5** (1977) 165.
18. N. C. BLAIS and J. J. VALENTINI, Preprint of the 8th Symposium (International) on Detonation, Albuquerque, New Mexico, USA, July 1985 (Lawrence Livermore, National Laboratory, USA 1985) Vol. 1, p. 425.
19. F. P. BOWDEN and M. M. CHAUDHRI, *Nature* **220** (1968) 690.
20. M. M. CHAUDHRI and J. E. FIELD, *Proc. R. Soc.* **A340** (1974) 113.
21. B. E. BARTLETT, F. C. TOMPKINS and D. A. YOUNG, *J. Chem. Soc.* 3323 (1956).
22. T. B. TANG and M. M. CHAUDHRI, *Proc. R. Soc.* **A369** (1979) 83.

*Received 2 May
and accepted 21 July 1986*